Materials Today: Proceedings 26 (2020) 189–192

Contents lists available at ScienceDirect

Materials Today: Proceedings

journal homepage: www.elsevier.com/locate/matpr

Microstructural analysis of the friction stir welded 1050-H14 and 5083-H111 aluminium alloys

Velaphi Msomi *, Nontle Mbana, Sipokazi Mabuwa

Department of Mechanical Engineering, Cape Peninsula University of Technology, Symphony Way, Bellvile 7535, South Africa

ARTICLE INFO

Article history:
Received 22 July 2019
Received in revised form 7 August 2019
Accepted 12 October 2019
Available online 2 November 2019

Keywords:
Friction stir welding
Aluminium alloys
Scanning electron microscopy
Microhardness
Tensile strength properties

ABSTRACT

Friction stir welding technique is considered to be the newly developed technique which was aimed at welding soft metals. The initial focus of this welding technique was on welding similar aluminium alloys. The focus expanded and included the dissimilar alloys and materials. This paper reports on the quality of the joint formed when 1050-H14 and 5083-H111 aluminium alloys were friction stir welded. The converted milling machine was utilized in performing the welding. The welded joint was then analysed in comparison with the parent materials. The correlation between the microstructural observations and the mechanical behaviour of the joint is thoroughly discussed in the main text of this paper.

Selection and peer-review under responsibility of the scientific committee of the 10th International Conference of Materials Processing and Characterization.

1. Introduction

Friction stir welding (FSW) is considered to be a fairly new welding technique which was developed to weld soft materials like copper and its alloys, aluminium and its alloys, etc. [1,2]. These soft metals were difficult to weld using the traditional welding techniques due to their low melting temperatures. The development of friction stir welding came as a solution mitigating this challenge [3]. Most of the early work that was reported around this technique involved the welding of similar materials and alloys [4,5]. Later, the technique was tested in welding dissimilar materials [6–8]. This involves two different materials or two different alloys [9,10]. The use of FSW in joining dissimilar materials is a subject that is currently under investing. There are couple of works that have performed in this area. The majority of the work on dissimilar materials involved the alloys that are not far apart from each other [11–13]. The recent works are now focusing on the optimization of FSW technique to weld dissimilar alloys that are widely apart from each other [14]. The welding of dissimilar alloys that are widely apart from each other require some certain welding parameters combinations and these combinations are different from the ones used in welding dissimilar alloys that are close to each other. There are numerous investigations that are being conducted in finding the different welding parameters combinations that are relevant to different dissimilar alloys [15,16].

The objective of this paper is to evaluate the mechanical properties of the friction stir welded widely apart aluminium alloys. In this study, the widely apart aluminium alloys used were 1050-H14 and 5083-H111.

2. Experimental procedure

The guillotine cutting machine was used to cut aluminium alloy 1050-H14 and 5083-H111 plates into 70 × 530 mm dimensions. The semi-automated milling machine was used to perform the welding of AA1050-H14 and AA5083-H111. The high carbon steel (H13) was used to manufacture the welding tool which was then heat treated to about 50HRB. The tool had a triangular threaded pin profile with a shoulder diameter of the 20 mm shoulder and the pin diameter of 6 mm. The length of the pin was 5.8 mm. The whole setup and the performance of friction stir welding is shown in Fig. 1. The tool rotational speed was set to be 1000 rpm while the clamped work pieces traversed with the speed of 30 mm/min. The tool tilt angle was set to be 2°. The chemical composition of the materials used in this study is shown in Table 1 [17].

The sample of the produced weld is shown in Fig. 2. The waterjet cutter was used to cut the dog-bone shaped tensile test specimens (shown in Fig. 3) perpendicular to the FSW progression direction. The specimens were cut in this fashion so as to ensure that the gauge length is located in the nugget location. The similar approach was used to cut specimens used for microstructural analysis. The waterjet cutter was chosen because it does not involve

* Corresponding author.
E-mail address: msomiv@gmail.com (V. Msomi).

https://doi.org/10.1016/j.matpr.2019.10.038
2214-7853/
Selection and peer-review under responsibility of the scientific committee of the 10th International Conference of Materials Processing and Characterization.

Fig. 1. Semi-automated milling machine.

Table 1
Chemical composition of AA1050-H14 and AA5083-T111 (wt%).

Material	Si	Fe	Cu	Mn	Mg	Cr	Zn	Ti	Al
AA1050-H14	0.10	0.29	0.01	–	0.02	–	0.01	0.02	Balance
AA5083-T111	0.14	0.20	0.01	0.65	4.62	0.10	0.01	0.01	Balance

Fig. 2. Sample of the FSW joint.

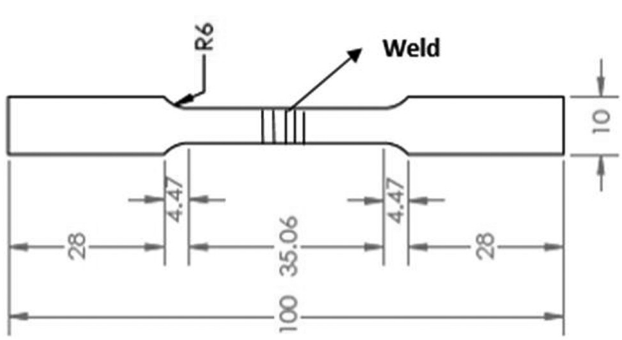

Fig. 3. Tensile test specimen.

temperature during cutting. The optical microscopy was used to analyse the microstructure of the nugget zone. The fracture analysis was performed on the post tensile test specimens through the use of Scanning Electron Microscopy (SEM).

Table 2
Tensile test results.

Specimen	Ultimate tensile strength (MPa)	Percentage elongation
A	50.67	8.4
B	66.47	11.34
C	63.19	11.4
BM1	104.89	6.6
BM2	326.75	26.7

3. Results and discussions

It should be noted that the friction stir welded joint had a start, middle and ending points and the specimens were cut in that order. The specimens cut in the start position were labelled A while B and C were indicating middle and the ending positions. The presentation of all results followed this particular fashion. It should be noted again that the welds were analysed in comparison with the base materials. The 1050-H14 base metal is referred as BM1 while 5083-H111 base metal is BM2.

The tensile test properties of the weld and base metals are presented in Table 2. The ultimate tensile stress (UTS) for the specimens extracted from the welded region were found to be the lower than the base metals (BM1 and BM2). The specimen B and C were considerable higher than the specimen A. The specimen B and C were found to be more ductile compared to specimen A and base metal 1050-H14. This ductility is judged from the percentage elongation of a material [18,19]. However, the ductility of base metal 5083-H111 was found to be relatively higher compared to all the specimens. The properties of the specimen A were observed to be lower than specimen B and C. This behavior is suggested to be caused by the insufficient heat input occurring at the beginning of the weld.

The fractured specimens from tensile testing were prepared for SEM analysis. Fig. 4 shows the fractured surface for BM1 and BM2 against specimen C. There was no difference in surface morphology between the fractured surfaces extracted from different locations of the weld hence only one weld specimen is presented against the base metals. All the specimens show a cup like dimpled fracture which is an indication of ductile failure mode [18,19]. The size of the dimples for the weld and the base metals was measured to be in the range between 6 μm and 22 μm. This suggests that the joint formed by ductile metals is also ductile. So the ductility of the materials was not affected post welding even though there were some variations that were shown by the tensile elongation percentage.

The Vicker's microhardness profile of the specimen C is shown in Fig. 5. The measurement was taken from the center to either sides of the specimen and this measurement was located 3 mm

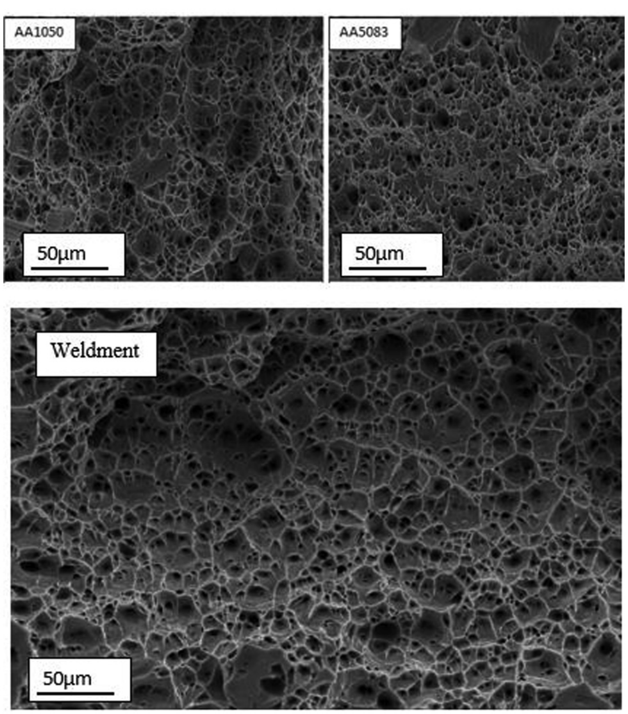

Fig. 4. Micrograph of the base metals and the welded specimen C.

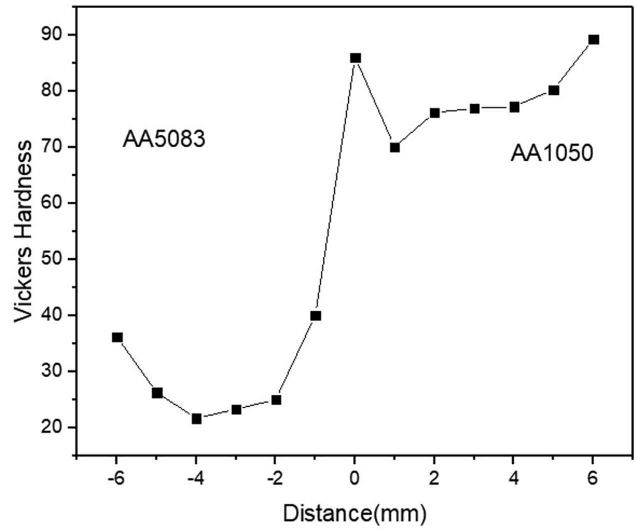

Fig. 5. Microhardness profile for specimen C.

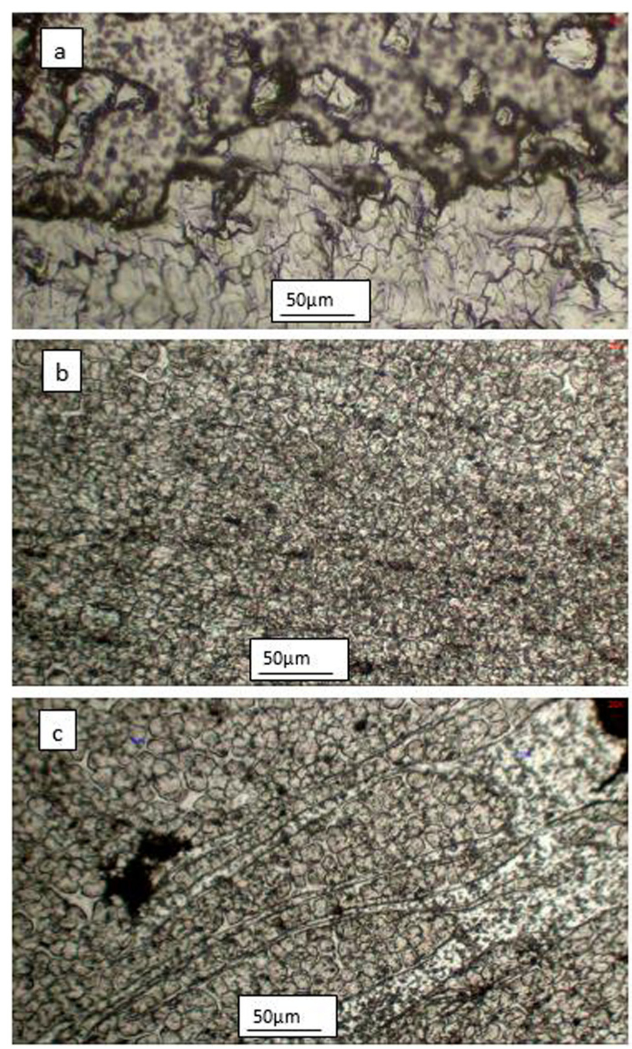

Fig. 6. Optical metallography images of (a) AA1050 base metal, (b) AA5083 base metal, (c) the stir zone.

from the root face of the sample. The indentation load used for the microhardness was 300 g. The Vicker's hardness for AA5083-H111 is about 80 while AA1050-H14 has the value of about 40. There is notable decrease in hardness value from the side of AA5083-H111 which then followed by the drastic increase towards the center of the weld. There is a notable decrease in hardness value from the center of the weld towards the side of AA1050-H14 and thereafter a sharp increase is noted towards the end of the weld. This behaviour suggests that the AA5083-H111 side was dominated by AA1050-H14 while AA5083-H111 dominated the side of AA1050-H14 post welding. This behaviour further indicates that the grain size of the weld towards the AA1050-H14 are smaller than those dominating AA5083-H111 side [17].

The optical metallographic images for AA1050-H14 base metal, AA5083-H111 base metal and stir zone are depicted in Fig. 6. The average grain size for AA1050-H14 were measured to be approximately 30–40 μm while the average grain size for AA5083-H111 was in the range of 6–8 μm and these ranges are in correlation with the values available in the literature [17]. The stir zone average grain size was measured and it was ranging between 6 and 11 μm. This range is not far off from the AA5083-H111 base metal. The morphology of the stir zone shows features similar to the morphology of AA5083-H111 base metal with some elongated whitish structures in between. The elongated whitish structures are the stir precipitates of AA1050-H14 that was pulled towards the AA5083-H111 side. These are the same structures that are normally categorized as the onion rings [4,9,12,13].

4. Conclusions

The friction stir welding was successfully performed on using 1050-H14 and 5083-H111 dissimilar aluminium plates under normal environmental conditions. The welded plates were analysed mechanically and microstructurally. The tensile properties of the joint were found to be higher than the tensile properties of AA1050-H14 base metal but lower than the properties of AA5083-H111 base metal. The microhardness of the stir zone was found to be higher than the AA1050-H14 base metal but at the same range with AA5083-H111 base metal. The grain size of the stir zone was in the range close to the AA5083-H111 base metal. The morphology of the stir zone also was similar to the one for AA5083-H111 base metal. The results for microhardness were found to be in agreement with the tensile properties.

Acknowledgements

The authors would like to thank Ms S Petersen for her assistance with the microstructural investigations. The authors would also like to thank Mr EM Masekwana for his assistance with the performance of the welding.

References

[1] R.S. Mishra, Z.Y. Ma, Mater. Sci. Eng. 50 (2005) 1–78.
[2] S.K. Tiwari, D.K. Shukla, R. Chandra, Int. J. Mech. Aerosp. Ind. Mechatron. Manuf.Eng. 7 (12) (2013) 1326–1331.
[3] V. Paradiso, F. Rubino, P. Carlone, G.S. Palazzo, Procedia Eng. 183 (2017) 239–244.
[4] A. Tongne, C. Desrayaud, M. Jahazi, E. Feulvarch, J. Mater. Process. Technol. 239 (2017) 284–296.
[5] P.L. Threadgill, A.J. Leonard, H.R. Shercliff, P.J. Withers, Int. Mater. Rev. 54 (2009) 49–93.
[6] S. Sheikhi, C. Bolfarini, J. Mater. Process. Technol. 206 (2008) 132–142.
[7] P. Sadeesh, P. Rajkumar, N. Avinash, K. Arivazhagan, S. Narayanan, Procedia Eng. 75 (2014) 145–149.
[8] J. Kundu, H. Singh, Eng. Sol. Mech. 4 (2016) 125–132.
[9] R. Ranjith, WSEAS Trans. Appl. Theor. Mech. 9 (2014) 179–186.
[10] L.I. Xia-wei, Z. Da-tong, Q.I.U. Cheng, Z. Wen, Trans. Nonferrous Met. Soc. China 22 (6) (2012) 1298–1306.
[11] N.T. Kumbhar, K. Bhanumurthy, J. Metal (2012) 7–10.
[12] U. Donatus, G.E. Thompson, X. Zhou, J. Wang, K. Beamish, Mater. Des. 83 (2015) 203–213.
[13] U. Das, V. Toppo, Mater. Today: Proc. 5 (5) (2018) 11556–11562.
[14] Y. Song, X. Yang, L. Cui, X. Hou, Y. Xu, Mater. Des. 55 (2014) 9–18.
[15] M.P. Jenarthanan, C. Varun Varma, V. Krishna Manohar, Mater. Today: Proc. 5 (6) (2018) 14384–14391.
[16] P. Hema, K. Sai kumar naik, K. Ravindranath, Mater. Today: Proc. 4 (2017) 2174–2183.
[17] S.Y. Sato, M. Urata, H. Kokawa, K. Ikeda, Mater. Sci. Eng. A 354 (2003) 298–305.
[18] G. D'Urso, C. Giardini, S. Lorenzi, T. Pastore, J. Mater. Process. Technol. 214 (2014) 2075–2084.
[19] J.F. Guo, H.C. Chen, C.N. Sun, G. Bi, Z. Sun, J. Wei, Mater. Des. 56 (2014) 185–192.